Geobiology (2007), **5**, 141–151 DOI: 10.1111/j.1472-4669.2007.00098.x

Rates of methanogenesis and methanotrophy in deep-sea sediments

O. SIVAN,[1] D. P. SCHRAG[2] AND R. W. MURRAY[3]

[1]*Department of Geological and Environmental Sciences, Ben Gurion University, Beer Sheva 84105, Israel*
[2]*Department of Earth and Planetary Sciences, Harvard University, 20 Oxford St., Cambridge, MA 02138, USA*
[3]*Department of Earth Sciences, Boston University, 685 Commonwealth Avenue, Boston, MA 02215, USA*

ABSTRACT

We use the carbon isotopic composition ($\delta^{13}C$) of the dissolved inorganic carbon (DIC) of pore fluids from Leg 175 of the Ocean Drilling Program (ODP) along the West African Margin to quantify rates of methane production (methanogenesis) and destruction via oxidation (methanotrophy) in deep-sea sediments. Results from a model of diffusion and reaction in the sedimentary column show that anaerobic methane oxidation (AOM) occurs in the transition zone between the presence of sulfate and methane, and methanogenesis occurs below these depths in a narrow confined zone that ends at about 250 m below the sea-sediments surface in all sediment profiles. Our model suggests that the rates of methanogenesis and AOM range between $6 \cdot 10^{-8}$ and $1 \cdot 10^{-10}$ mol cm^{-3} year^{-1} at all sites, with higher rates at sites where sulfate is depleted in shallower depths. Our AOM rates agree with those based solely on sulfate concentration profiles, but are much lower than those calculated from experiments of sulfate reduction through AOM done under laboratory conditions. At sites where the total organic carbon (TOC) is less than 5% of the total sediment, we calculate that AOM is the main pathway for sulfate reduction. We calculate that higher rates of AOM are associated with increased recrystallization rates of carbonate minerals. We do not find a correlation between methanogenesis rates and the content of carbonate or TOC in the sediments, porosity, sedimentation rate, or the C:N ratio, and the cause of lack of methanogenesis below a certain depth is not clear. There does, however, appear to be an association between the rates of methanogenesis and the location of the site in the upwelling system, suggesting that some variable such as the type of the organic matter or the nature of the microbiological community may be important.

Received 29 October 2006; accepted 04 January 2007

Corresponding author: O. Sivan. Tel.: 972-8-6477504; fax: 972-8-6472997; e-mail: oritsi@bgu.ac.il.

INTRODUCTION

Deep-sea sediments are the largest reservoir of methane (CH_4), which occurs mainly as hydrate (~10^7 TgC). The current emission from CH_4 hydrates to the atmosphere is small (~10 Tg year^{-1}), compared to both anthropogenic (~350 Tg year^{-1}) and other natural sources such as wetlands (~110 Tg year^{-1}) (IPCC, 2001; Wuebbles & Hayhoe, 2002). Although the release from methane hydrate is currently small, many scientists estimate that in Earth history there could have been large, catastrophic releases of methane from hydrates, resulting in abrupt increases in global temperature. One possible example of this is the terminal Palaeocene, 55 Ma (e.g. Zachos *et al.*, 1993; Dickens *et al.*, 1995; Bice & Marotzke, 2002). In addition, some studies have proposed that gas hydrates may be used as an energy source (e.g. Kvenvolden, 1988).

Most of the methane in sediments is produced in organic-rich areas by bacterial methanogenesis under anaerobic conditions (Martens & Berner, 1974). The general belief is that the mechanism for this biotic methane formation in marine sediments is reduction of CO_2, which is produced from organic matter fermentation (e.g. Belyaev *et al.*, 1977; Whiticar *et al.*, 1986). However, there are few works suggesting that acetate is an important substrate for methanogenesis (e.g. Parkes *et al.*, 2000). Acetate fermentation is the dominant pathway for methanogenesis in terrestrial sediments (Whiticar *et al.*, 1986).

Methane is dissolved in deep-sea pore fluids, and is supersaturated depending on pressure and temperature conditions. When methane diffuses upwards in marine sediments, it is oxidized (methanotrophy) under anaerobic conditions by sulfate in a molar ratio of 1 : 1, mediated probably by consortia

of archaea and sulfate-reducing bacteria (e.g. Boetius *et al.*, 2000; Orphan *et al.*, 2001, 2002):

$$SO_4^{2-} + CH_4 \xrightarrow{archaea,bacteria} HCO_3^- + HS^- + H_2O \quad (1)$$

The first geochemical evidence for this anaerobic oxidation of methane (AOM) process came from depth distributions of CH_4 concentrations in anoxic organic-rich marine sediments (Barnes & Goldberg, 1976; Reeburgh, 1976; Martens & Berner, 1977). These studies showed that high CH_4 concentrations do not occur unless dissolved SO_4^{2-} has been depleted to concentrations of less than 1.0 mM. Diagenetic models have demonstrated that 'concave up' CH_4 concentration profiles can only be explained by consumption of methane in the transition zone with SO_4^{2-} (Reeburgh, 1976; Barnes & Goldberg, 1976; Martens & Berner, 1977; Scranton, 1988). Direct rate measurements using radiotracers (e.g. Reeburgh, 1980; Hoehler *et al.*, 1994), and the distributions of stable isotopes, their budgets, and fractionation factors provided further evidence of AOM (e.g. Whiticar *et al.*, 1986; Alperin *et al.*, 1988).

The AOM process was initially controversial among microbiologists because neither the responsible organism nor the mechanism had yet been identified. Recently, geomicrobiologists showed that a consortium of archaea and bacteria are involved in AOM in some seep environments (Hoehler & Alperin, 1996; Hinrichs *et al.*, 1999; Boetius *et al.*, 2000; Orphan *et al.*, 2001). The methane oxidizers have not yet been grown in pure culture.

The AOM process increases the alkalinity of the porewater and therefore may result in co-precipitation of carbonate minerals (Moore *et al.*, 2004). However, the importance of AOM is mainly the sharp transition zone between SO_4^{2-} and CH_4 that is created, where the downward diffusive flux of sulfate should equal that of the upward diffusion of methane if all of both sulfate and methane are consumed solely through AOM. AOM thus acts to limit the methane flux toward the sediment–water interface, explaining the low emission from marine sediments (Borowski *et al.*, 1996). The transition zone between CH_4 and SO_4^{2-} can occur in the upper few centimeters of the sediments (Martens & Berner, 1977; Martens *et al.*, 1999; Boetius *et al.*, 2000) or at greater depths (tens of meters, e.g. Borowski *et al.*, 2000; D'Hondt *et al.*, 2002).

Even though several studies have estimated the flux of methane toward the AOM zone (e.g. Reeburgh, 1980; Sansone & Martens, 1981; Hoehler *et al.*, 1994; Borowski *et al.*, 1996; Niewöhner *et al.*, 1998), the rates of both methanogenesis and AOM for the same marine (and also terrestrial) sediments, and their variation with depth, have not been well quantified. In this paper, we quantify the rates of methanogenesis and methanotrophy in deep-sea sediments by modelling the processes affecting the carbon isotopic composition ($\delta^{13}C$) of the dissolved inorganic carbon (DIC) in the porewater. We show that $\delta^{13}C_{DIC}$ provides a good constraint on the rates of methanogenesis and AOM because of the large isotopic fractionation associated with methanogenesis, our ability to calculate the other reaction rates and the model sensitivity to the best fits and isotopic fractionations.

Methanogenesis results in isotopically depleted methane, with values ranging mostly between –50 and –80‰ PDB in marine sediments (Whiticar *et al.*, 1986; Burke *et al.*, 1988; Martens *et al.*, 1999), and a much heavier pool of DIC due to fractionation effect of about 60‰ (e.g. Whiticar, 1999; Borowski *et al.*, 2000). AOM affects $\delta^{13}C_{DIC}$ values by oxidizing almost all the isotopically depleted methane to DIC. The fractionation is therefore small (less than 10‰, e.g. Coleman & Risatti, 1981; Alperin *et al.*, 1988; Martens *et al.*, 1999; Borowski *et al.*, 2000), and it is due to the light isotope ^{12}C that is oxidized more rapidly than the heavy isotope, ^{13}C, enriching the residual methane in ^{13}C (Coleman & Risatti, 1981; Orphan *et al.*, 2004). Aside from AOM, sulfate reduction by oxidation of organic matter adds DIC with $\delta^{13}C$ values of the oxidized organic matter (~–21‰ PDB in this type of sediments (Lin *et al.*, 2001). Dissolution of carbonate minerals adds DIC with $\delta^{13}C$ values of the carbonate, and precipitation of carbonate minerals removes porewater DIC with little fractionation (+2‰ PDB, e.g. Faure, 1986). Our approach of modelling $\delta^{13}C_{DIC}$ profiles is an alternative to incubation experiments at high pressure or rate calculations based solely on methane measurements, which can have large errors due to escape during cores handling (e.g. Paull *et al.*, 2000).

METHODS

Sites description

We used pore fluid data from sediments collected in Leg 175 of the ODP along the West African Margin (Wefer *et al.*, 1998). The Angola-Benguela Current system is one of the great upwelling regions of the world. Sediments are largely diatomaceous and carbonate-rich clays with variable high organic carbon content (3–8%). Authigenic minerals, such as dolomite, are present. The drilled sites are at water depths ranging from 400 to 2200 m. Methane is found at all sites, but below saturation, so no methane gas or gas hydrates exist. Typical porosity is 70–80% at the top of the sediment, with small variation throughout the bottom of the cores (decreasing slightly to 50–60% at a sediment depth of ~500 m). Sedimentation rates at the sites are between 5 and 20 cm kyr^{-1} (Wefer *et al.*, 1998).

Sites 1075, 1076 and 1077 (Lower Congo Basin) contain the record of sediment supply by the Congo River intercalated with oceanic record. The high sedimentation rates at sites 1078 and 1079 (Mid-Angola Basin) are influenced by a supply of silt from coastal erosion. Site 1080 (Southern Angola Basin) is located in the northern end of the Angola–Namibia upwelling region. Site 1081 is affected by variability in seasonal coastal upwelling and by the supply of dust from

Namib Desert. Sediments at this site consist of grey clays with varying amounts of diatoms, nannofossils, foraminifers and radiolarians. Sites 1082, 1083 and especially 1084 lie close to the major upwelling centers along south-west Africa with year-round upwelling activity. Site 1084 has high sedimentation rates (10–27 cm kyr^{-1}), high productivity and high rates of phytoplankton accumulation. Sites 1085, 1086 and 1087 (Mid-Southern Cape Basins) are influenced by seasonal upwelling and continental input to the sediment (Wefer *et al.*, 1998).

Sampling and measuring

Cores were collected with advanced hydraulic piston corers (APC) and extended core barrel (XCB) at deep sediments. Major ions, total alkalinity and methane concentrations in the porewater were measured on board using standard ODP methods and the headspace method for methane (Murray *et al.*, 1998). As previously mentioned, measurements of methane concentrations are suspected to have large errors due to escape during cores handling, and therefore our calculations were not based on them. Porewater samples for $\delta^{13}C_{DIC}$, the carbon isotopic composition of the DIC ($\delta^{13}C(‰) = (({}^{13}C/{}^{12}C)_{sample} - ({}^{13}C/{}^{12}C)_{std}) * 1000/({}^{13}C/{}^{12}C)_{std}$), were poisoned with $HgCl_2$ after squeezing and kept in vacutainer vials. The samples were acidified with orthophosphoric acid before the measurement, and the evolved CO_2 was measured on an Optima gas-source isotopic ratio mass spectrometer at the Laboratory for Geochemical Oceanography at Harvard University (Moore *et al.*, 2004). The error of these isotopic measurements, based on replicate measurements and analysis of laboratory standards, is ±0.1‰.

Modelling

A mass conservation numerical model that describes the porewater depth profiles of $\delta^{13}C_{DIC}$ was constructed for this study. The basic conservation equation for the concentration of a chemical species i in porewater ($M \cdot L^{-3}$, where M is the mass and L is the length) has a general form, as described by Berner (1980) that includes terms for diffusion, sedimentation advection and reactions, respectively:

$$\frac{\partial C_i}{\partial t} = \frac{\partial}{\partial z}\left(Ds_i \frac{\partial C_i}{\partial z}\right) - (U + \omega)\frac{\partial C_i}{\partial z} + \sum R_i \qquad (2)$$

where z is depth within the sediment column (L); t is time (T); ϕ is porosity; and D_s is the diffusion coefficient of dissolved species i in sediments ($L^2 \cdot T^{-1}$), where we assumed that $D_{s(i)} \sim D_{0(i)} \cdot \phi^2$ (after Lerman, 1979) and D_0 is the diffusion coefficient of dissolved species i in seawater (values calculated after Berner, 1980); U is the advection term ($L \cdot T^{-1}$); ω is the sedimentation rate ($L \cdot T^{-1}$); and ΣR is the sum of the reaction rates of the dissolved species i by a variety of diagenetic processes.

Since the variation in the porosity is small (0.7 ± 0.1, Wefer *et al.*, 1998), we assumed a constant porosity along the profiles, which simplified the mathematical expression (making $D_{0(i)} \cdot \phi^2$ constant). This simplification has only a minor affect on the results, and is small compared with the total error. In addition, the large gradients in the major ion profiles and the shape of their curves indicate that there is not significant advection of water in these sediments. The simplified conservation equation is therefore:

$$\frac{\partial C_i}{\partial t} = DS_i \frac{\partial^2 C_i}{\partial z^2} - \omega \frac{\partial C_i}{\partial z} + \sum R_i \qquad (3)$$

Equation 3 was solved numerically through finite difference with 1-m boxes and time steps of 10 years, with bottom seawater values as the upper boundary condition, and nonflux condition at the bottom of the sediments. The initial conditions were constant sulfate concentrations with seawater values all along the sediments and the absence of methane. As the conditions evolved, the profiles changed until the steady state profiles were obtained (methane was allowed to appear when sulfate concentrations were below 1 mM).

The chemical and biological reactions included in the model were those that can add or remove DIC from the porewater and therefore affect the $\delta^{13}C_{DIC}$ profile: dissolution and precipitation of carbonate minerals, anaerobic oxidation of organic matter oxidation (OMO), methane oxidation by sulfate reduction (AOM), methanogenesis and a currently unknown sink for methane below the zone of methanogenesis (which affects only CH_4 profiles). Sulfate and methane concentrations, as well as $^{12}C_{DIC}$ and $^{13}C_{DIC}$ (allowing the calculation of $\delta^{13}C_{DIC}$), were individually tracked in our model. The $^{13}C_{DIC}$ concentration was calculated at each depth from the $^{12}C_{DIC}$ value and the fractionation factor for each chemical or biological reaction described above with their natural variations. In addition, Ca^{2+} and Mg^{2+} concentrations were modelled as the sum of the two cations ($Ca^{2+} + Mg^{2+}$) to simplify the treatment of carbonate minerals (i.e. we did not distinguish between dolomite and calcite). Ca^{2+} and Mg^{2+} concentrations and the dissolution and precipitation of carbonate phases are treated more fully in Moore *et al.* (2004).

The reaction function terms were based on the following assumptions. First, that the rate of AOM is proportional to sulfate and methane concentrations with a 1 : 1 molar ratio as previously determined by models and measurements ($k[CH_4][SO_4^{2-}]$, e.g. Borowski *et al.*, 1996; Martens *et al.*, 1999; Nauhaus *et al.*, 2002). That means that the rate has a maximum at the transition zone between sulfate and methane. Second, that the rate of methanogenesis can have a variety of profiles, including a maximum at a certain depth z ($Az \cdot e^{-Bz}$). Third, that the precipitation rate of carbonate minerals has a maxima at the depth of the observed intensive precipitations from the profiles of Ca^{2+} and Mg^{2+} (proportional to z of max

methanogenesis and max AOM). The dissolution rate of carbonate minerals was set to balance the DIC changes with changing methane concentrations. The function rate for organic matter oxidation by sulfate followed Berner (1980). The reaction rates were calculated by running the model forward until steady state conditions were achieved. The functions and the rate coefficients were iterated until the best fits to the measurements were obtained, and the sensitivity of the model to the best fits and fractionation variations was tested.

Alternatively, we solved equation 3 for steady state conditions ($\partial(species)/\partial t = 0$) to calculate the rates in each depth, and obtained similar results. In this case the solution was simplified, also with our calculations that the sedimentation term was neglectable compared to diffusion:

$$C_{i(z+1)} = -C_{i(z-1)} + 2C_{i(z)} - \frac{\Delta z^2}{Ds_i} \sum R_i \qquad (4)$$

This numerical solution did not require any function assumptions for the rates as when we solved equation 3 using finite difference. Instead, the absolute rates were calculated at each depth. The first step in this way was to determine the concentration of each species in each box (1 m) from interpolation of the data according to a best-fit curve. Then, the net dissolution rate of Ca + Mg minerals (dissolution minus precipitation) was found in each depth from the Ca + Mg best-fitted profile and its equation solution. Organic matter oxidation by sulfate above the methane zone was calculated from sulfate best-fit curve and its equation solution. These calculations enabled us then to determine the absolute rates of methanogenesis or AOM at each depth using two equations, one for ^{12}C and one for ^{13}C, with two unknown parameters (gross dissolution and AOM or methanogenesis). We use Site 1081 for a series of sensitivity tests, and present the best-fit results from other sites from Leg 175.

RESULTS

Profiles description

The physical properties, major ion profiles, and part of the $\delta^{13}C_{DIC}$ profiles of the different sites in Leg 175 have been previously shown (available in Murray *et al.*, 1998; Wefer *et al.*, 1998; Moore *et al.*, 2004). Table 1 summarizes the main characteristics of each site, and we here summarize the pore-fluid characteristics of the most relevant species for this study, using Site 1081 as a representative example. At Site 1081, SO_4^{2-} concentrations in the porewater decrease due to bacterial sulfate reduction from around 26.5 mM near the sediment–water interface to its complete depletion at around 60 m (Fig. 1A). CH_4 starts to appear below 55 m due to methanogenesis, and its concentration increases to a maximum of 12.5 mM at about 100 m. Below 250 m, CH_4 concentrations are less than 1 mM throughout the bottom of the sediments (450 m, Fig. 1B). Ca^{2+} concentrations decrease sharply in the upper part of the sediments from 10.5 mM to 3.5 mM at approximately 50 m. Below 100 m its concentrations increase slightly and remain high through the bottom of the core (Fig. 1C). Mg^{2+} concentrations also decrease sharply in the upper 100 m from 52.5 mM to 30.5 mM (Fig. 1C). These two profiles, and their sum ($Ca^{2+} + Mg^{2+}$), indicate that there are two zones of significant carbonate mineral precipitation, at ~55 and ~100 m (Fig. 1C). The pH of the porewater increases from 7.5 at the top sediments to a maximum value of about 8.0 at 55 m, then decreases to a minimum value of ~6.5 at 100 m, and remains near 7.0 below 120 m (Fig. 1D). Total alkalinity increases from about 4 mM at the top of the sediments to a maximum value of about 30 mM at 200 m with a local maximum at 50 m and a minimum at 100 m (Fig. 1E). DIC concentrations were calculated from the pH and the alkalinity (assuming that the alkalinity is mostly carbonate alkalinity) and are very close to the measured alkalinity

Table 1 Main characteristics of the sites in Leg 175 of the Ocean Drilling Project (ODP) (after Wefer *et al.*, 1998; Moore *et al.*, 2004)

Site	Water depth (m)	Upper sed. rate (cm kyr^{-1})	Average porosity (%)	Sulfate depletion depth (m)	Depth of maximum methane (m)	Methane maximum concentration (mM)	Depth of minimum calcium (m)	Calcium minimum maximum (mM)	Upper depth of maximum alkalinity (m)	Alkalinity maximum concentration (mEq L^{-1})	Depth of lightest $\delta^{13}C_{DIC}$ (m)	$\delta^{13}C_{DIC}$ lightest values (‰ PDB)
1075	3000	20	80	31	63	13	31	5	42	40	30	–29.0
1076	1400	31	80	28	66	16	57		43	36	28	–28.0
1077	2390	21	80	30	67	12	38	5	76	37	28	–28.0
1078	440	25	60	20	31	12	21	3	68	74	15	–23.0
1079	750	35	70	50	50	9	57	3			38	–27.0
1080	2780	4	80	6	9	5			9	41	6	–25.0
1081	800	7	70	60	93	12	43	3	67	25	51	–21.5
1082	1290	7	70	25	34	19	35	3	35	47	19	–20.5
1084	2000	27	80	7	26	15	17	4	45	143	6	–9.1
1085	1710	4	60	50	100	10	46	3	50	27	45	–19.0
1086	790	5	60	180		0					160	–5.0
1087	1390	3	60	70	100	2					70	–9.0

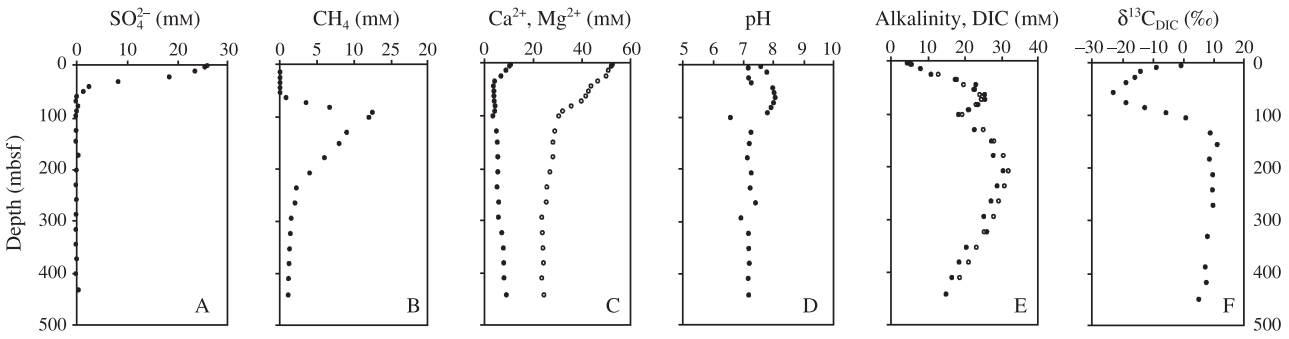

Fig. 1 Porewater data profiles at site 1081 of SO_4^{2-} (A), CH_4, where its concentrations are less than 15% from saturation (calculated from Zhang, 2003). (B), Ca^{2+} (filled circles) and Mg^{2+} (empty circles) (C), pH (D), total alkalinity (filled circles) and calculated dissolved inorganic carbon (DIC), assuming that the alkalinity is mostly carbonate alkalinity (empty circles) (E), and $\delta^{13}C_{DIC}$ (F) (after Wefer *et al*., 1998; Moore *et al*., 2004).

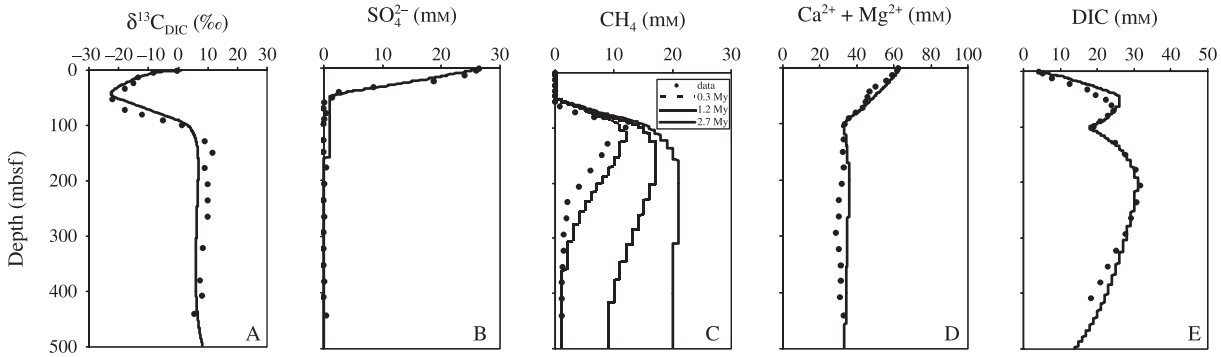

Fig. 2 Data (filled circles) and model results at steady state (curves) at site 1081 of $\delta^{13}C_{DIC}$ (a quasi steady state was achieved already after 0.5 Myr) (A), SO_4^{2-} (steady state was achieved after 0.5 Myr) (B), CH_4 in run time of 0.3–2.7 Myr (C), $Mg^{2+} + Ca^{2+}$ (D), and dissolved inorganic carbon (DIC) (E). These model curves are calculated taking into consideration diffusion, sedimentation and reactions with the restriction that CH_4 is absent in the sulfate zone. Steady state was achieved when the profile has stabilized and stopped to change.

values (Fig. 1E). $\delta^{13}C_{DIC}$ decreases significantly in the sulfate reduction zone from about 0‰ at the top of the sediments to −22‰ at 55 m. Below the sulfate–methane transition zone, $\delta^{13}C_{DIC}$ starts to increase due to methanogenesis, reaching its maximum value of about +10‰ at below 100 m, and then levels off throughout the bottom of the core (Fig. 1F).

Modelling

The best-fit curves at Site 1081 for all species were achieved first by running the forward model until steady state conditions were reached using the assumed reaction functions discussed above. In these conditions, a quasi steady state for $\delta^{13}C_{DIC}$ was achieved after 0.5 Myr (Fig. 2A), meaning that after that time the profiles had not been changed. A steady state for SO_4^{2-} was achieved after 0.5 Myr (Fig. 2B), meaning that after this time the model reproduced the data profile, and for CH_4, $Mg^{2+} + Ca^{2+}$ and DIC after ~2 Myr (Fig. 2C–E). These results were achieved using the isotopic effect from the literature of less than 10‰ for AOM and +60‰ for methanogenesis. $\delta^{13}C_{CH4}$ was estimated to be −50‰ from the $\delta^{13}C_{DIC}$ values at the methane zone (+10‰) and from the isotopic fractionation of carbon isotopes during methanogenesis.

The AOM and methanogenesis rate profiles used to achieve the best-fit curves are presented in Fig. 3 (similar results obtained from the 'steady state solution'). Our model calculations confirm that AOM is likely confined to the sulfate–methane transition zone, with a maximum rate of methanotrophy of $\sim 7 \cdot 10^{-10}$ mol cm^{-3} year^{-1} at about 50 m (Fig. 3). Methanogenesis occurs below the sulfate–methane transition zone in a confined zone with a maximum rate of $5 \cdot 10^{-10}$ mol cm^{-3} year^{-1} at about 100 m (where $\delta^{13}C_{DIC}$ reaches its maximum value). Our calculations also suggest that rates of methanogenesis are insignificant below 200 m (Fig. 3). The rate of precipitation of carbonate minerals is very low throughout most of the sediment column (about $5 \cdot 10^{-11}$ mol cm^{-3} year^{-1}), about $3 \cdot 10^{-10}$ mol cm^{-3} year^{-1} around 50 m depth, and about $20 \cdot 10^{-10}$ mol cm^{-3} year^{-1} around 100 m depth. These are the same depths where concentration profiles suggest that maximum of AOM and methanogenesis occur. We calculate that the dissolution rates of carbonate mineral are less than

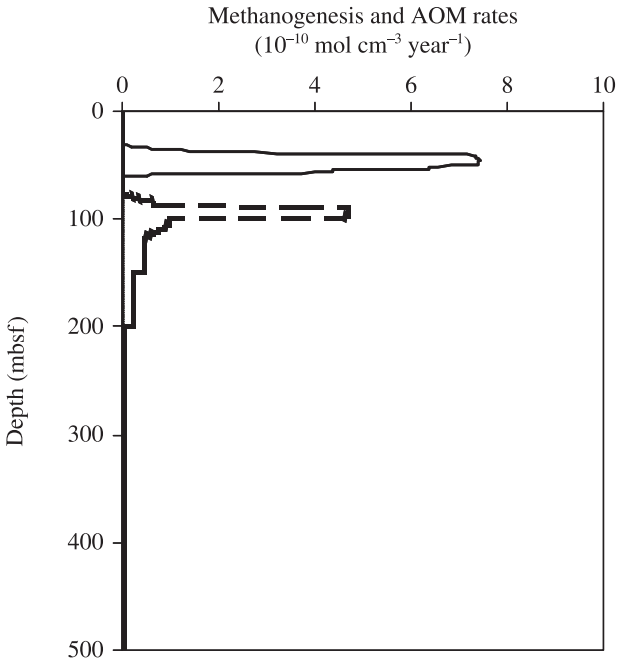

Fig. 3 Modelled anaerobic methane oxidation (solid line) and methanogenesis (dashed line) rate profiles in steady state conditions.

$5 \cdot 10^{-11}$ mol cm^{-3} year^{-1} and relatively constant with depth, and therefore the net carbonate precipitation rate values (precipitation minus dissolution) are essentially the precipitation rate. Modelled CH_4 profiles are similar to observations in the upper part of the sediment column. However, below 100 m, while the data show a significant decrease of CH_4 with sediment depth, CH_4 continues to accumulate in the model, creating a misfit (Fig. 2C). When we added a process in the model that consumes only methane (i.e. it almost does not release DIC), we obtained a reasonable fit to the methane data in steady state conditions with a constant sink of ~$2.5 \cdot 10^{-11}$ mol cm^{-3} year^{-1} between 200 and 360 m (Fig. 4) or smaller rates on larger depth range. The precipitation rates of carbonate minerals are very low throughout the sediments, except for around 50 m (about $3 \cdot 10^{-10}$ mol cm^{-3} year^{-1}) and 100 m depth ($20 \cdot 10^{-10}$ mol cm^{-3} year^{-1}), the zones of maximum AOM and maximum methanogenesis, respectively. The slight changes in the dissolution rates of carbonate minerals needed to balance the methane concentrations did not affect the other profiles, and kept the net precipitation rate (or recrystallization) similar to the rate of absolute precipitation.

A sensitivity test was performed on the model results from Site 1081 to determine the uncertainty of our model calculations, investigating all the possible best-fits and fractionation variations. For example, when the rates of methanogenesis were changed by 70% and the maximum depth of methanogenesis by 20 m, the best fit of $\delta^{13}C_{DIC}$ to the data in the AOM/methanogenesis zone decreased from $R^2 = 0.9$ to $R^2 = 0.6$. We estimate, based on the fit of the model to the $\delta^{13}C_{DIC}$ data, that the error in our calculated rates is approximately 50% in magnitude and ±20 m in depth. It seems, therefore, that $\delta^{13}C_{DIC}$ profile, combined with SO_4^{2-}, Mg^{2+}, Ca^{2+} and DIC profiles, provides a good constraint on the rate processes involving methane, considering the variations in the concentrations and the isotopic fractionations.

Methane was found in significant concentrations in almost all the sites (except Site 1086) of Leg 175 and, therefore, the same modelling approach was used in all these sites. Our calculations show that in all the sites containing methane, except Site 1084, sulfate reduction rate by organic matter oxidation is minor compared to AOM. Therefore, AOM is responsible for reducing the majority of the sulfate pool in most of the sediments off the west coast of Africa, as was concluded also from other work at that area (Niewohner *et al.*, 1998). At all sites, we calculate that AOM occurs at the transition zone between methane and sulfate, and methanogenesis occurs below that zone in a narrow confined zone that ends above

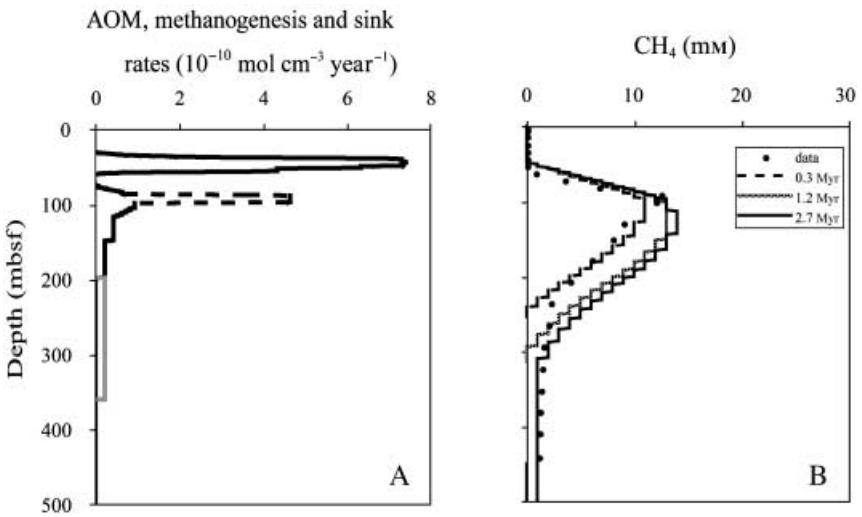

Fig. 4 Modelled anaerobic methane oxidation (solid black line), methanogenesis (dashed line) and deep sink (solid grey line) methane rate profiles in steady state conditions (A), and the best-fit curves of CH_4 achieved in this case for different run times (B).

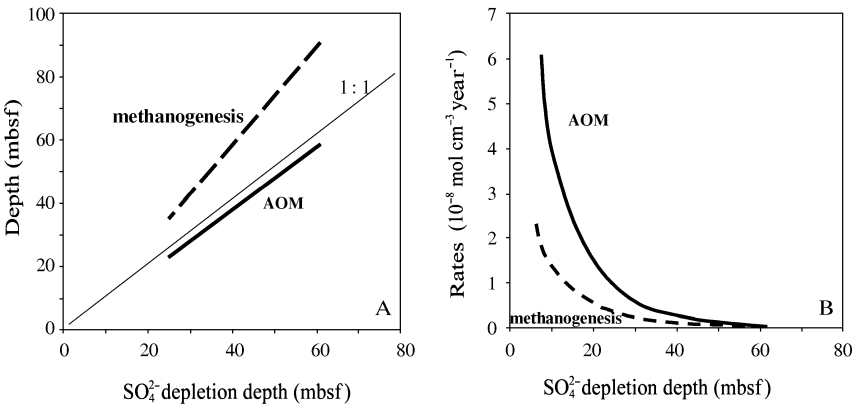

Fig. 5 Modelled anaerobic methane oxidation and methanogenesis depths of maximum rates (A) and the maximum rates in those depths (B) from the various sites of Leg 175.

250 m. The sites are different in their rates of methanogenesis and AOM and their depth distribution. The rates of AOM and methanogenesis range between $6 \cdot 10^{-8}$ and $1 \cdot 10^{-10}$ mol cm^{-3} year^{-1}, where higher rates are located at shallower depths (few meters) and lower rates at deeper depths (Fig. 5). Our model results suggest that both AOM and methanogenesis are accompanied by recrystallization of carbonate minerals.

DISCUSSION

The different rate profiles at the various sites emphasize the coupling between methanogenesis and AOM and the correlation with sulfate depletion depth. In general, increasing rates of methanogenesis result in an increase in the diffusive flux of methane toward the transition zone. This increasing flux moves the sulfate–methane transition zone to a shallower depth where the diffusive flux of sulfate equals that of methane. Therefore, higher rates of methanogenesis and AOM (and in shallower depths) are found at sites where the sulfate is depleted in shallower depths (Fig. 5).

Anaerobic methane oxidation (AOM) by sulfate reduction

The concave-up shape of sulfate profiles in the upper few meters of the sediments at Site 1081 (Fig. 1A) and at other sites records slight sulfate reduction and reoxidation in the uppermost few meters of sediment. Below this zone and until the transition zone with methane, there is almost a linear decrease of sulfate with depth. The linear decrease suggested for Site 1081 is observed clearly in the high resolution profiles of the other sites of Leg 175 (such as Site 1082, Wefer *et al.*, 1998) and in other studies that have produced very high-resolution sulfate concentration profiles (e.g. Borowski *et al.*, 1996; Niewohner *et al.*, 1998). The linear nature of the sulfate concentration profiles indicates that diffusion is the dominant process affecting sulfate concentrations at any given depth. It means also that sulfate reduction becomes dominant only close to the methane transition zone, and that sulfate is consumed almost entirely by methane (as concluded also by Niewohner *et al.* (1998) based on short profiles off the coast of Namibia). Indeed, at almost all sites, $\delta^{13}C_{DIC}$ values in the sulfate–methane transition zone were explained in our model by AOM alone without additional oxidation of organic matter (which has an average $\delta^{13}C$ of ~−21‰ PDB (Lin *et al.*, 2001)). These values were not lighter than ~−25‰, because of the diffusive flux of 'heavy' carbon from the methanogenesis zone and the upper part, and due to carbonate minerals dissolution. Our flux calculations at Site 1081 emphasize this finding. Based on the concentration profiles of sulfate and methane, and the linear curve close to the transition zone, we calculate that the downward diffusive flux of sulfate toward this zone is close to the upward diffusive flux of methane. These fluxes close to the integrated rate of AOM based on our $\delta^{13}C_{DIC}$ model calculations ($7 \cdot 10^{-7}$ mol cm^{-2} year^{-1}) and confirm our calculations. Using these rates, the model reproduced sulfate data profile after 0.5 Myr. Our finding that AOM is the dominant process for sulfate reduction in all but one of the 12 sites is surprising, if we consider the traditional view on sulfate reduction by organic matter. However, it was shown previously in other sediments around the world (Reeburgh, 1980; Sansone & Martens, 1981; Borowski *et al.*, 1996; Niewohner *et al.*, 1998), and is further explored by us.

Our rates of AOM agree with previous calculations done in similar conditions (Borowski *et al.*, 2000; D'Hondt *et al.*, 2002). In these studies, AOM rates were calculated for shallow- and deep-water environments and both from SO_4^{2-} and CH_4 profiles (flux calculations based on concentration gradients) and from laboratory studies. The experimental studies documenting rates of AOM have included mainly radiotracers, inhibition and incubation studies (e.g. Hoehler *et al.*, 1994; Martens *et al.*, 1999; Boetius *et al.*, 2000; Nauhaus *et al.*, 2002). AOM maximum rates in shallow gassy rich organic coastal sediments were $15 \cdot 10^{-6}$ mol cm^{-3} year^{-1} at ~30 cm sediment depth, both from radiotracer experiments and from flux calculations, and a first-order rate reaction constant for AOM of 8 year^{-1} was determined (Martens *et al.*, 1999). AOM maximum rates in a shallow barrier island lagoon were ~$3 \cdot 10^{-6}$ mol cm^{-3} year^{-1} at ~30 cm sediment depth in the

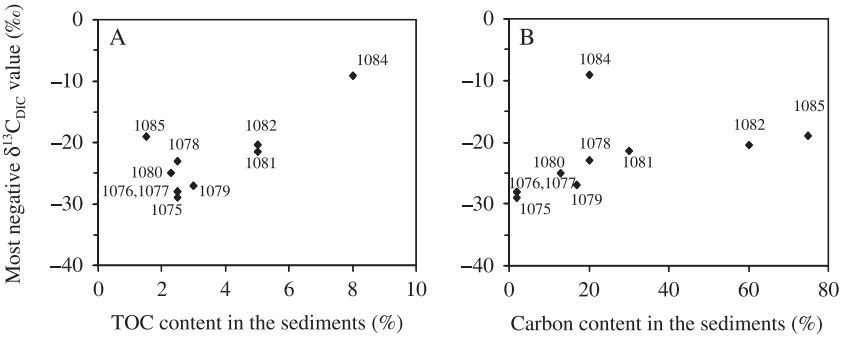

Fig. 6 The most negative values of $\delta^{13}C_{DIC}$ at different sites of Leg 175 vs. the concentrations of the total organic matter (wt%) from the total sediments at these sites (A), and vs. the concentrations of the carbonate (wt%) from the total sediments at these sites (B).TOC, total organic carbon.

winter, and ~$6 \cdot 10^{-6}$ mol cm^{-3} year^{-1} at ~10 cm sediment depth in the summer (Hoehler & Alperin, 1996). A maximum SO_4^{2-} reduction rate of more than $2 \cdot 10^{-3}$ mol cm^{-3} year^{-1} at ~1 cm sediment depth was measured at the Cascadian hydrate ridge (780 m water depth) and was explained by AOM (Boetius *et al.*, 2000). AOM rates in the Blake Ridge (2780 m water depth) calculated from CH_4 flux were $5 \cdot 10^{-9}$ mol cm^{-3} year^{-1} at ~21 m sediment depth (Borowski *et al.*, 2000). SO_4^{2-} fluxes due to AOM were about $6 \cdot 10^{-7}$ mol cm^{-2} year^{-1} at 30 m depth in the sediments, and $1 \cdot 10^{-6}$ mol cm^{-2} year^{-1} at 10 m depth in the sediments (D'Hondt *et al.*, 2002). Taken together, these studies confirm our modelled rates of AOM and methanogenesis and are consistent with our finding that higher rates of methanogenesis and AOM are found at sites where the sulfate is depleted in shallower depths.

The reduction of sulfate mainly by methane suggests that the organic matter is less available to sulfate-reducing bacteria than are the oxidation products of methane. The one exception to this in Leg 175 is Site 1084. At this site, our calculated upward methane flux toward the transition zone (based on the AOM rate profile and methane concentration profile) is around $3 \cdot 10^{-6}$ mol cm^{-2} year^{-1}, whereas the integrated rate profile of sulfate reduction by organic matter oxidation suggests downward flux of $6 \cdot 10^{-6}$ mol cm^{-2} year^{-1}, and the total downward flux of sulfate is $1 \cdot 10^{-5}$ mol cm^{-2} year^{-1}. Therefore, at this site, our calculations suggest that 30% of the sulfate is reduced by methane and the rest by organic matter. Site 1084 is different from the other sites by its relatively heavy $\delta^{13}C_{DIC}$ values in the sulfate–methane transition zone (the depth of most negative $\delta^{13}C_{DIC}$ values) and the high amount of organic matter (~8wt%). This would suggest that there is an apparent association between the minimum $\delta^{13}C_{DIC}$ value at a given site and the content of total organic carbon (TOC) in the sediments at that site (Fig. 6A). This implies that the organic matter is more labile and more available to sulfate-reducing bacteria when there is more organic matter.

The variations in $\delta^{13}C_{DIC}$ values at the sulfate–methane transition zone among the sites of Leg 175 with relatively low organic matter, where sulfate is reduced mainly by methane, seem to be associated with the carbonate content. Sites with higher concentrations of carbonate mineral have greater gross rates of carbonate dissolution and precipitation (more effect of the carbonate minerals) and therefore more positive $\delta^{13}C_{DIC}$ values (Fig. 6B). AOM, in general, releases HCO_3^- to the porewater, and therefore increases the alkalinity and the pH, resulting in precipitation of carbonate minerals, as indicated by the profiles (Fig. 1E). Layers of organogenic dolomite, dolomite that is precipitating due to diagenetic processes (Compton & Siever, 1986; Mazzullo, 2000), were indeed observed in these sediments and were related to AOM (Moore *et al.*, 2004).

Methanogenesis

We calculate that methanogenesis at all sites is confined to a narrow zone below the zone of AOM and above 250 m with a maximum at a given depth (Fig. 5). There does not seem to be a correlation between methanogenesis rates and TOC or the concentrations of the carbonate in the sediments, porosity, sedimentation rate, or C/N ratio. There is an association between the rates of methanogenesis and the location of the site along the African Coast, with higher rates of methanogenesis at the upwelling region off the coast of Namibia. This suggests that some variable such as the type of the organic matter in that area or the nature of the microbiological community producing the organic matter supplied to the sediment may be important. It should be noted that even though it appears that the organic matter is unavailable to the sulfate-reducing bacteria, it becomes available to methanogens at greater depths. To the extent that sulfate reduction and methanogenesis require the same substrates, this finding requires further investigation at both the sulfate zone and the methanogenesis zone.

The reason for the lack of methanogenesis at greater depths than 250 m is also not clear, as the TOC content does not appear to decrease with depth in the sediment, suggesting ample supply of 'food' for methanogenesis to continue throughout the core. One reason might be related to the oxidation state of the organic matter, which can affect its reactivity, making it inactivate in the sediments. Another factor that could be changed at a certain depth is the structure of the microbiological community. Methanogenesis may also be

inhibited by one of the dissolved species other than sulfate, such as CH_4 itself, as the product of this process.

Another observation that is hard to explain is that the highest rates of carbonate mineral precipitation are associated with the 100 m peak in methanogenesis. While AOM is expected to increase alkalinity and precipitate carbonates, the net process of methanogenesis from organic matter should not. The pH values are consistent with the rate peaks; maximum at the AOM zone (pH = 8.0, Wefer *et al.*, 1998), where bicarbonate is released, and minimum at the peak of methanogenesis (pH = 6.56, Wefer *et al.*, 1998). It should be noted that the AOM carbonate minerals peak is driven principally by Ca precipitation, while the 100 m peak is driven by Mg precipitation.

The best-fit curves for all species except methane were achieved by assuming steady state conditions and by using methanogenesis and AOM (by sulfate) as the main reactions involving methane. We were not able to model CH_4 profiles in any of the sites using these conditions, because the model could not reproduce the decrease of CH_4, observed in at least seven sites, at greater depths (profiles in Wefer *et al.*, 1998). A decrease in methanogenesis is not enough to produce this CH_4 decrease as that would suggest only constant methane concentrations below 100 m. We were able to obtain a reasonable fit to the methane data by allowing the model to run for only 0.5–0.8 Myr. This could be interpreted as implying that methane began to accumulate in the sediments 0.5–0.8 Ma. However, since a similar decrease in CH_4 profiles is observed at other sites around the world as well [e.g. Leg 164 – Blake Nose and Carolina Rise (Paull *et al.*, 1996), Leg 172 – North–west Atlantic Sediment Drift (Borowski *et al.*, 2000), Leg 204 – Cascadia Margin (Bohrmann *et al.*, 2002)], it seems unlikely that methane started accumulating at all these sites 0.5–0.8 Ma.

Methane loss during core handling of the deeper cores is the most reasonable explanation for an 'apparent' decrease in methane concentrations with depth, because of the extreme pressure decrease (and therefore decrease in the saturation level of CH_4), using the headspace method (e.g. Paull *et al.*, 2000). Since this method is problematic, efforts have been made to design pressure core samplers (PCS) that can measure accurately the concentrations of gas hydrate and free gas (e.g. Dickens *et al.*, 1997, 2000). Recent PCS profiles from Leg 204 (Bohrmann *et al.*, 2002) emphasize clearly the large discrepancy between the PCS and the headspace methods. Whereas PCS methane concentrations are compatible with the shallower headspace methane estimates, they become much higher than the headspace concentrations at greater depths, with values at or above saturation (within the gas hydrate stability zone).

It can be seen therefore, that the headspace method underestimates methane concentrations, and indeed, we have not used these measurements to calculate methanotrophy and methanogenesis rates. However, there are some indications that the headspace pattern (at least below saturation, like in Leg 175) might indicate in some processes. First, we did not find any correlation between the methane-decreasing depth and the pressure. That means that CH_4 concentrations continue to increase at some sites of Leg 175, much above the pressure in which CH_4 decrease was observed in Leg 164 and 204, using the same headspace method. It should be noted also that methane 'drop' depth, in most cases, is in the zone of the APC coring, and is not related to the changing of the coring method to XCB in greater depths. However, it is correlated to the sulfate depletion depth and methanogenesis maximum rate depth. In addition, as described above, the upward diffusive flux of methane, calculated from the headspace concentrations of methane, was equal to the downward flux of sulfate, calculated from sulfate profile, and to the fluxes calculated from $\delta^{13}C_{DIC}$ model (in similar pressures to the drop depth). There might be a decrease pattern also in the PCS data of Leg 204, however, it is not significant.

Based on these considerations, it can be also speculated that methane decrease is related to a process that consumes methane but does not affect the $\delta^{13}C_{DIC}$ profiles. A possible sink of methane that would not affect $\delta^{13}C_{DIC}$ profile could be a microbially mediated polymerization process that uses CH_4 and an electron acceptor (like ferric iron) to make higher alkanes in high efficiency (i.e. low CO_2 release). The lighter C_2–C_4 compounds that are direct products of polymerization reactions may only be intermediates and ultimately incorporated into higher alkanes.

When a sink of methane of $2.5 \cdot 10^{-11}$ mol cm^{-3} year^{-1} is added to the model at site 1081 between 200 and 360 m, a reasonable fit to the data is achieved (Fig. 4). This rate matches the downward diffusive flux of methane from modelled methanogenesis rates (flux ~$1 \cdot 10^{-7}$ mol cm^{-2} year^{-1}). The depth distribution of this sink is reasonable, as it starts below the methanogenesis zone and ends when methane is depleted (Fig. 4). Although any discussion of a deep sink for methane will be highly speculative given the uncertainty in the measurements of methane concentrations, it is interesting to further explore this possibility, attempting to find a solid evidence for this process.

CONCLUSIONS

Methane concentrations are significant at almost all the sites of Leg 175. In these sites, AOM occurs in the transition zone between sulfate and methane, and methanogenesis occurs below these depths in a narrow confined zone. Methanogenesis and AOM rates off the west coast of Africa range between $6 \cdot 10^{-8}$ and $6 \cdot 10^{-10}$ mol cm^{-3} year^{-1}, where higher rates are found at sites where the sulfate is depleted in shallower depths. In most sites, the organic matter is less available to the sulfate-reducing bacteria than the methane, and methane reduces almost the whole pool of sulfate. In those sites, the variations in $\delta^{13}C_{DIC}$ values are associated with the rates of carbonate recrystallization. Our AOM rates agree

with those based solely on sulfate profiles, and are much lower than those calculated from the sulfate reduction rate experiments due to AOM under laboratory conditions. Methanogenesis rates and depth distributions are not correlated to the concentrations of the carbonate or the TOC in the sediments, porosity, sedimentation rate, or C/N ratio. The ending of this process might be related to other (new?) microbial communities that out-compete the methanogens.

ACKNOWLEDGEMENTS

We thank A. Pearson for helpful discussions, and the anonymous reviewers for their comments that greatly improved this manuscript. This work was funded by OCE-0452329 grant for DP Schrag and the Bikura fellowship for O. Sivan.

REFERENCES

Alperin MJ, Reeburgh WS, Whiticar MJ (1988) Carbon and hydrogen fractionation resulting from anaerobic methane oxidation. *Global Biogeochemical Cycles* **2**, 279–288.

Barnes RO, Goldberg ED (1976) Methane production and consumption in anoxic marine sediments. *Geology* **4**, 297–300.

Belyaev SS, Laurinavichus KS, Gaytan VI (1977) Modern microbial formation of methane in Quarternary and Pliocene rocks of the Caspanian Sea. *Geochemistry International* **4**, 172–176.

Berner RA (1980) *Early Diagenesis: A Theoretical Approach.* Princeton University Press, Princeton, New Jersey.

Bice KL, Marotzke J (2002) Could changing ocean circulation have destabilized methane hydrate at the Paleocene/Eocene boundary? *Paleoceanography* **17**, 10.1029/2001PA000678.

Boetius A, Ravenschlag K, Schubert CJ, Rickert D, Widdel F, Gieseke A, Amann R, Jbrgensen BB, Witte U, Pfannkuche O (2000) A marine consortium apparently mediating anaerobic oxidation of methane. *Nature* **407**, 623–626.

Bohrmann G, Trehu AM, Rack FR, Shipboard Scientific Party (2002) *Ocean Drilling Program, Preliminary Report* **204**, Texas A&M University, College Station, TX, USA.

Borowski WS, Paull CK, Ussler W III (1996) Marine pore fluid sulfate profiles indicate in situ methane flux from underlying gas hydrate. *Geology* **24**, 655–658.

Borowski WS, Cagatay N, Ternois Y, Paull CK (2000) Data report: carbon isotopic composition of dissolved CO_2, CO_2 gas, and methane, Blake-Bahama Ridge and northeast Bermuda Rise, ODP Leg 172. *Proceedings of the Ocean Drilling Program, Scientific Results* **172**. http://www-odp.tamu.edu/publications/172_SR/chap_03/chap_03.htm.

Burke RA, Martens CS, Sackett WM (1988) Seasonal variations of D/H and 13C/12C ratios of microbial methane in surface sediments. *Nature* **332**, 829–831.

Coleman DD, Risatti JB (1981) Fractionation of carbon and hydrogen isotopes by methane-oxidizing bacteria. *Geochemica Cosmochemica Acta* **45**, 1033–1037.

Compton JS, Siever R (1986) Diffusion and mass balance of Mg during early dolomite formation, Monterey Formation. *Geochemica Cosmochemica Acta* **50**, 125–135.

D'Hondt S, Rutherford S, Spivack AJ (2002) Metabolic activity of subsurface life in deep-sea sediments. *Science* **295**, 2067–2070.

Dickens GR, O'Neil JR, Rea DK, Owen RM (1995) Dissociation of oceanic methane hydrate as a cause of the carbon isotope excursion at the end of the Paleocene. *Paleoceanography* **10**, 965–971.

Dickens GR, Paull CK, Wallace P, The ODP Leg 164 Scientific Party (1997) Direct measurement of situ methane quantities in a large gas-hydrate reservoir. *Nature* **385**, 426–428.

Dickens GR, Wallace P, Paull CK, Borowski WS (2000) Detection of methane gas hydrate in the Pressure Core Sampler (PCS): volume-pressure-time relations during controlled degassing experiments. In *Proceedings of the Ocean Drilling Program, Scientific Results* (eds Paull CK, Matsumoto R, Wallace PJ, Dillon WP).Vol. 164, pp. 113–126, Texas A&M University, College Station, TX, USA.

Faure G (1986) *Principles of Isotope Geology*. Wiley, New York.

Hinrichs K-U, Hayes JM, Sylva SP, Brewer PG, DeLong EF (1999) Methane-consuming archaebacteria in marine sediments. *Nature* **398**, 802–805.

Hoehler TM, Alperin MJ, Albert DB, Martens CS (1994) Field and laboratory studies of methane oxidation in anoxic marine sediment: evidence for a methanogen-sulfate reducer consortium. *Global Biogeochemical Cycles* **8**, 451–463.

Hoehler TM, Alperin MJ (1996) Anaerobic methane oxidation by a methanogen-sulfate reducer consortium: geochemical evidence and biochemical considerations. In *Microbial Growth on C-1 Compounds* (eds Lidstrom ME, Tabita RF). Kluwer Academic Publishing, Dordrecht, the Netherlands. pp. 326–333.

Intergovernmental Panel on Climate Change (IPCC) (2001) In *Climate Change 2001: The Scientific Basis, Contribution of Working Group 1 to the Third Assessment Report of the Intergovernmental Panel on Climate Change* Ch. 4. Atmospheric chemistry and greenhouse gases. (eds Houghten JT, Ding Y, Griggs DJ, Noguer M, Linden PJVD, Dai X, Maskell K, Johnson CA). Cambridge University Press, Cambridge, UK. pp. 241–280.

Kvenvolden K (1988) Methane hydrates and global climate. *Global Biochemical Cycles* **3**, 221–229.

Lerman A (1979) *Migrational Processes and Chemical Reaction in Interstitial Waters, Geochemical Processes in Water and Sediment Environments*. Wiley Interscience, New York.

Lin H, Lin C, Meyers PA (2001) Data report: carbonate, organic carbon, and opal concentrations and organic d13C values of sediments from sites 1075–1082 and 1084, Southwest Africa margin. *Proceedings of the Ocean Drilling Program Scientific Results* **175** http://www-odp.tamu.edu/publications/175_SR.

Martens CS, Albert DB, Alperin MJ (1999) Stable isotope tracing of anaerobic methane oxidation in the gassy sediments of Eckernforde Bay, German Baltic Sea. *American Journal of Science* **299**, 589–610.

Martens CS, Berner RA (1974) Methane production in the interstitial waters of sulfate-depleted marine sediments. *Science* **185**, 1167–1169.

Martens CS, Berner RA (1977) Interstitial water chemistry of anoxic Long Island Sound sediments, I, dissolved gases. *Limnology and Oceanography* **22**, 10–25.

Mazzullo SJ (2000) Organogenic dolomitization in peritidal to deep-sea sediments. *Journal of Sediment Research* **70** (1), 10–23.

Moore TS, Murray RW, Kurtz AC, Schrag DP (2004) Anaerobic methane oxidation and the formation of dolomite. *Earth and Planetary Science Letters* **229**, 141–154.

Murray RW, Wigley R, Shipboard Scientific Party (1998) Interstitial water chemistry of deeply buried sediments from the Southwest African Margin: a preliminary synthesis of results from Leg 175. *Proceedings of the Ocean Drilling Program in Initial Report* **175**, 547–553.

Nauhaus K, Boetius A, Kruker M, Widdel F (2002) In vitro demonstration of anaerobic oxidation of methane coupled to sulfate reduction in sediment from a marine gas hydrate area. *Environmental Microbiology* **4**, 296–305.

Niewöhner C, Hensen C, Kasten S, Zabel M, Schulz HD (1998) Deep sulfate reduction completely mediated by anaerobic methane

oxidation in sediments of the upwelling area off Namibia. *Geochimica et Cosmochimica Acta* **62** (3), 455–464.
Orphan VJ, House CH, Hinrichs K-U, McKeegan KD, DeLong EF (2001) Methane-consuming archaea revealed by direct coupled isotopic and phylogenetic analysis. *Science* **293**, 484–487.
Orphan VJ, House CH, Hinrichs K-U, McKeegan KD, DeLong EF (2002) Multiple archaeal groups mediate methane oxidation in anoxic cold seep sediments. *Proceedings of the National Academy of Sciences of the USA* **99** (11), 7663–7668.
Orphan VJ, Ussler W, IIINaehr TH, House CH, Hinrichs K-U, Paull CK (2004) Geological, geochemical, and microbiological heterogeneity of the seafloor around methane vents in the Eel River Basin, offshore California. *Chemical Geology* **205**, 265–289.
Parkes RJ, Cragg BA, Wellsbury P (2000) Recent studies on bacterial populations and processes in marine sediments: a review. *Hydrogeological Reviews* **8**, 11–28.
Paull CK, Lorenson TD, Dickens G, Borowski WS, Ussler W III, Kvenvolden K (2000) Comparisons of *in situ and* core gas measurements in ODP Leg 164 bore holes. *Annals of the New York Academy of Sciences* **912**, 23–31.
Paull CK, Matsumoto R, Wallace P, Shipboard Scientific Party (1996) *Proceedings of the Ocean Drilling Program Initial Report* **164**. Texas A&M University, College Station, TX, USA.
Reeburgh WS (1976) Methane consumption in Cariaco Trench waters and sediments. *Earth and Planetary Science Letters* **28**, 337–344.
Reeburgh WS (1980) Anaerobic methane oxidation: rate depth distributions in Skan Bay sediments. *Earth and Planetary Science Letters* **47**, 345–352.
Sansone FJ, Martens CS (1981) Methane production from acetate and associated methane fluxes from anoxic coastal sediments. *Science* **211**, 707–709.
Scranton MI (1988) Temporal variation in the methane content of the Cariaco Trench. *Deep Sea Research Part A* **35**, 1511–1523.
Wefer G, Berger WH, Richter C, Shipboard Scientific Party (1998) *Proceedings of the Ocean Drilling Program Initial Report* 175 [CD-ROM] Available from Ocean Drilling Program. Texas A&M University, College Station, Texas.
Whiticar MJ (1999) Carbon and hydrogen isotope systematics of bacterial formation and oxidation of methane. *Chemistry Geology* **161**, 291–314.
Whiticar MJ, Faber E, Schoell M (1986) Biogenic methane formation in marine and freshwater environments: CO_2 reduction vs. acetate fermentation – Isotope evidence. *Geochimica et Cosmochimica Acta* **50**, 693–709.
Wuebbles DJ, Hayhoe K (2002) Atmospheric methane and global change. *Earth-Science Review* **57**, 177–210.
Zachos JC, Lohmann KC, Walker JCG, Wise SW (1993) Abrupt climate change and transient climates in the Paleocene: a marine perspective. *Journal of Geology* **100**, 191–213.
Zhang Y (2003) Methane escape from gas hydrate systems in marine environment, and methane-driven oceanic eruptions. *Geophysical Research Letters* **30** (7), 1398. doi: 10.1029/2002GL016658.